



MGI's DNBSEQ Platform based RNA-seq Reveals Cell Junctions Regulate Vitellogenin Uptake in *Anguilla australis*

A Brief Introduction to One Research Empowered by the MGIEasy RNA Directional Library Prep Kit

The Department of Zoology at the University of Otago, New Zealand, conducted RNA-Seq of eel (*A. australis*) ovarian tissues using the MGI DNBSEQ sequencing platform to investigate the role of cell junction proteins in regulating the uptake of Vitellogenin (Vtg). By comparing the transcriptomes of pre-vitellogenic (PV) and early vitellogenic (EV) ovaries, they found that gene expression patterns may help identify suitable genes involved in regulating Vtg uptake and provided new sequencing data for *A. australis*. The related findings were published in the *Cells* journal in 2022 under the title "Are Cell Junctions Implicated in the Regulation of Vitellogenin Uptake? Insights from an RNAseq-Based Study in Eel, *Anguilla australis*".

Recommended application: Marine Genomics

Recommended model: DNBSEQ-G400RS

- A complete RNA-Seq solution

The MGIEasy RNA Directional Library Prep Kit can be used in combination with MGI's automation system, DNBSEQ sequencing platform and bioinformatics analysis software to empower RNA-Seq research.

- Efficient and high-quality sequencing data output

DNBSEQ sequencing technology exhibits many excellent features such as high accuracy, low repeat rate and low index hopping rate.

- Obtaining novel gene information related to Vtg uptake regulation

A *de novo* transcriptome assembly of the eel (*Anguilla australis*), and a RNA-seq based study on pre-vitellogenic (PV) and early vitellogenic (EV) ovaries have yielded novel gene information that may be involved in the regulation of Vtg uptake.



Background

In oviparous animals, the embryos develop and mature independently outside the maternal body, making high-quality eggs essential for the successful development of offspring². Ovarian development in oviparous animals involves three stages: the oogonia stage, pre-vitellogenic (PV) stage, and early vitellogenic (EV) stage^{3, 4}. Vitellogenesis is crucial for oocyte development, as it involves the uptake of a substantial amount of vitellogenin (Vtg), the precursor to vitellin (Vn), which rapidly accumulates in the oocyte. This accumulation provides energy reserves and abundant nutrients for subsequent embryonic development⁴.

The eel (*Anguilla australis*) is a bony fish species with a unique life cycle and serves as an ideal model for studying reproductive physiological regulation mechanisms⁵. In fishes, Vtg is primarily synthesized in the liver under the induction of estrogen and is transported to the ovaries through the bloodstream. Vtg uptake into oocytes is mediated by the Vtg receptor (VTGR), and VTGR is a unique factor affecting Vtg uptake. Various molecular events within the ovarian follicle also influence Vtg uptake. Therefore, the hypothesis of mechanical and chemical barriers has been proposed to investigate whether cell junctions are involved in the regulation of Vtg uptake.

Research Description

The Department of Zoology at the University of Otago, New Zealand, employed the MGIEasy RNA Directional Library Prep Kit (16RXN) on the MGI's DNBSEQ sequencing platform to construct the total RNA library for the ovarian tissues of *Anguilla australis*, followed by high-throughput sequencing. They compared the transcriptomes from pre-vitellogenic (PV) and early vitellogenic (EV) ovarian tissues in wild *Anguilla australis* using an RNA-seq based method. The findings identified 5 downregulated and 2 upregulated genes among the 25 genes encoding tight junction (TJ) proteins within the granulosa cell layer and support the mechanical barrier hypothesis. Furthermore, it was observed that the endocytic pathway was upregulated during the PV-EV transition. In conclusion, this study indicated that gene expression patterns may aid in identifying suitable genes involved in regulating Vtg uptake and provided new sequence data for *A. australis*, including putative Vtg receptors corresponding to members of the low-density lipoprotein receptor family, Lr8 and Lrp13.

Materials and Methods

Sample collection and RNA extraction

The research team captured wild short-finned eels from Lake Ellsemere at South Island, New Zealand in 2019. They were identified as pre-vitellogenic (PV) and early vitellogenic (EV) eels based on morphological features. The total body weight was measured, and the ovaries and liver were weighed after dissection to calculate somatic indices: Gonadosomatic Index (GSI) and

Hepatosomatic Index (HSI). Ovarian fragments were fixed in 4% paraformaldehyde for histological analysis and rapidly frozen for RNA extraction and next-generation sequencing.

Library preparation and sequencing

Total RNA was extracted from ovaries using the NucleoSpin RNA kit following the instructional manual. Then, the total RNA concentration was measured and the relative purity was determined, with a 260/280 nm absorbance ratio of about 2. Agilent 5300 was used to further assess the quality and integrity of RNA: RNA Integrity Numbers (RIN) was 7.1 ± 1.5 (PV stage, $n = 6$) and 10 (EV stage, $n = 6$).

Total RNA was constructed into strand-specific cDNA library using the MGIEasy RNA Directional Library Prep Kit V2.1 from MGI, followed by high-throughput sequencing. The brief steps are as follows: the mRNA in samples was first enriched with oligo-dT, and then fragmented, and reverse transcribed; after adapter ligation and PCR amplification, cDNA libraries were transformed into DNA nanoballs for paired-end 100 bp (PE100) sequencing on the DNBSEQ platform.

Bioinformatics Analysis and identification of target genes

Data quality was assessed using FastQC v0.11.9, and *de novo* transcriptome assembly was performed with Trinity v2.84.5. Ovarian developmental stages (PV/EV) were specified for each sample in Trinity. The raw reads were processed

using the align_and_estime.pl script from Trinity. Reads were aligned using Bowtie v1.2.0, and quantification was performed at the gene level using RSEM v1.3.2 and SAMtools v1.8. Transdecoder v5.5.0 was used to identify candidate coding regions in the assembled transcript sequences. Using Trinotate v3.2.1, in combination with the information from BLASTx and BLASTp from the UniProtKB/SwissProt database, to conduct functional annotation.

The target genes (GJs and TJs) encoding the proteins that make up cell junctions, and genes involved in endocytosis mediated by clathrin, intracellular vesicle trafficking, and Vtg processing were searched on the annotated transcriptome. The deduced protein sequences were retrieved, while the names of genes corresponding to *Anguilla australis* were searched through NCBI-BLASTp, and differential expression (DE) analysis was performed. In cases where multiple gene IDs were associated with the same functional annotation for filtered genes, only one gene ID was used based on the highest

read count, unless they were confirmed to correspond to different gene sequences after nucleotide and protein alignments. In addition, after using DeSeq2 v1.26.0 for count transformation, gene heatmaps related to the Vtg uptake pathway were visualized with the R package pheatmap v1.0.12.

The complete open reading frame of Vtgr was used to deduce the corresponding protein sequences, and the CD-Search tool on NCBI was used to analyze its conserved domain database before phylogenetic analysis. In order to construct a phylogenetic tree, amino acid sequences of members of the LDLR family (Low-Density Lipoprotein Receptor 8, LR8; Low-Density Lipoprotein Receptor-Related Protein 13, Lrp13; Low-Density Lipoprotein Receptor-Related Protein 4, LRP4) from different species were retrieved from NCBI. After aligning the sequences with the ClustalW algorithm, a phylogenetic tree was constructed using the Maximum Likelihood method in MEGA v7.

Sample collection	Library preparation and sequencing	Bioinformatics analysis	Result analysis
Short-finned eels from Lake Ellsemere	 MGIEasy RNA Directional Library Prep Set V2.1  Genetic Sequencer DNBSEQ-G400	Trinity Bowtie RSEM SAMtools Transdecoder DeSeq2 ClustalW MEGA etc.	The confirmation of genes involved in Vtg regulation

Results

Characteristics of Ovarian Development Stages

As the transition from the PV stage to the EV stage occurred, GSI, HIS, and OD significantly increased. Further histological analysis of ovaries confirmed the developmental stages based on morphological characteristics. Compared to PV oocytes, the oocytes in the EV stage showed a substantial increase in size due to the accumulation of lipid droplets and vitellogenin (Vtg incorporation). PV oocytes showed only a small amount of lipid droplets, and there were no signs of Vtg accumulation in their cytoplasm (Figure 1).

De novo transcriptome and downstream analysis

An average of 14.25 million reads of PE100/sample on the DNBSEQ platform generated a total of 282,469 transcripts from 171,620 putative

genes. Of these, 25.6% were functionally annotated. After low-expressed genes were filtered out, functional annotations were assigned to 64.1% (20,810) of the remaining 32,447 genes. Initial clustering analysis revealed that samples clustered into two distinct phenotypic categories, PV and EV.

During the PV-EV transition, the expression of genes related to three biological processes (endocytosis, membrane organization, and cation transmembrane transport regulation) and one molecular function (potassium channel inhibitor activity) was upregulated. In contrast, there were 15 downregulated gene categories across various GO groups, primarily associated with RNA metabolism and eggshell formation. Finally, a total of 4,878 genes showed differential expression, with 2,851 genes upregulated and 2,027 genes downregulated as the stage progressed from the PV to the EV stage (Figure 2 and Figure 3).

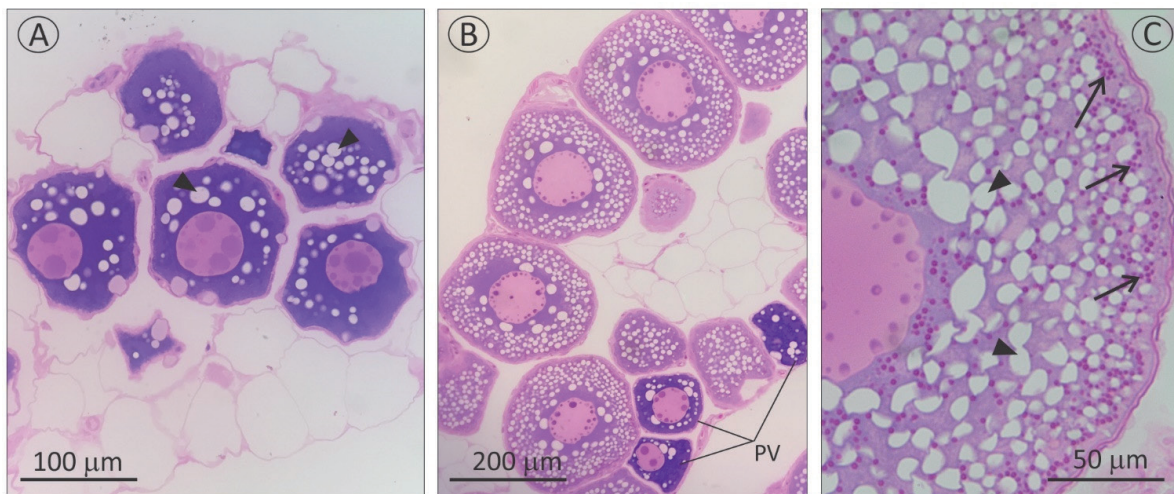


Figure 1. Histological sections of the ovaries of wild eels (2019) at the pre-vitellogenic stage (PV: (A)) and early vitellogenic stage (EV: (B,C)). The significant increase in oocyte size and the presence of vitellogenin (Vtg) (arrows) distinguish the EV stage from the PV stage. As shown in (B), EV ovaries typically contain few PV oocytes. Black arrowheads indicate lipid droplets.

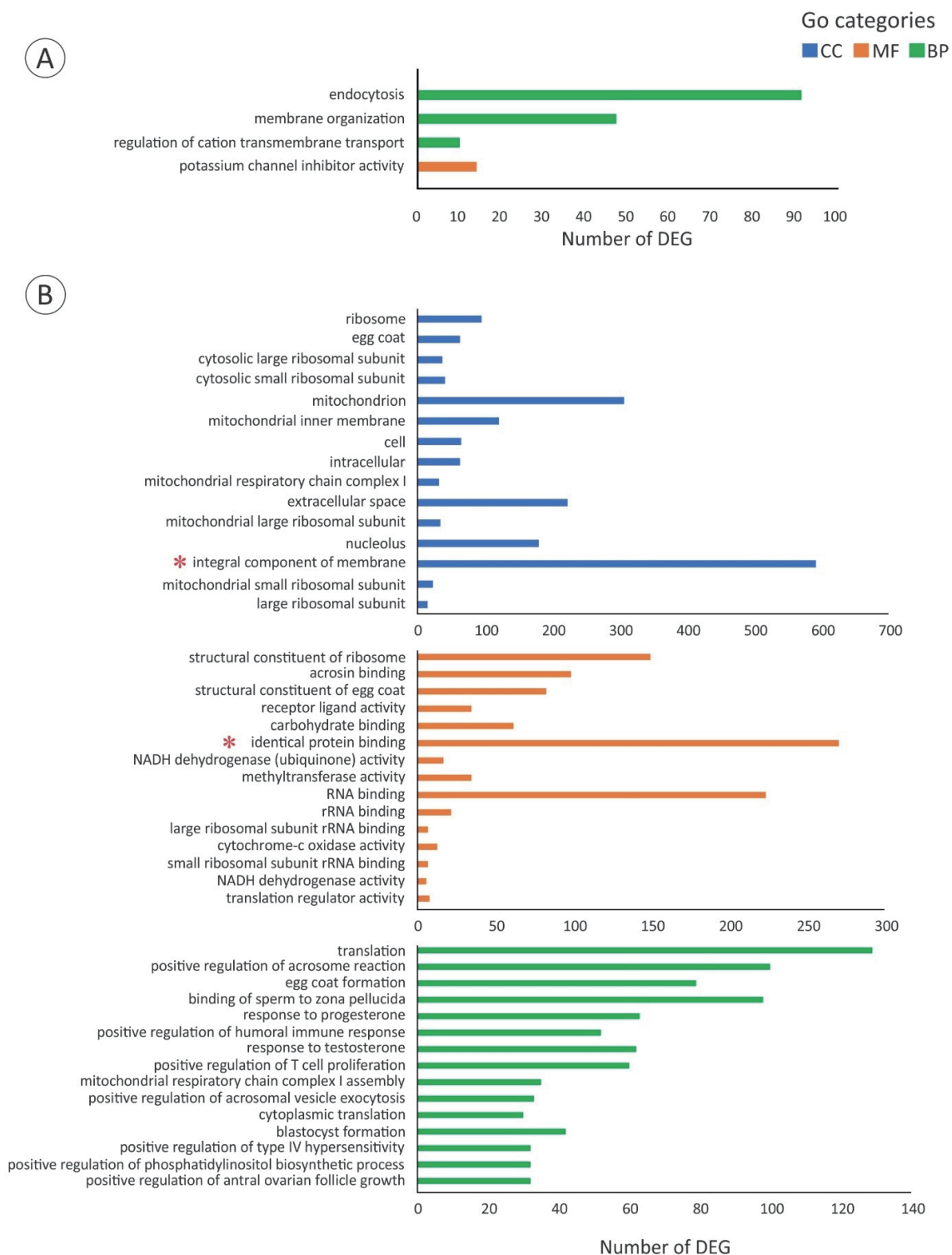


Figure 2. (A) All the GO terms that show upregulation in the ovary of *A. australis* progressing from the PV to the EV. (B) 15 down-regulated GO terms from Biological Process (BP), Molecular Function (MF), and Cellular Component (CC) categories during the PV-EV transition. Notably, terms related to the integral component of the membrane and identical protein binding are marked with a red asterisk.

Gene expression of cell junctions during the PV-EV transition

Of the 25 identified genes encoding various types of TJ-constituting proteins, seven genes exhibited differential expression. During the transition from the PV to the EV stage, only two genes were upregulated, while five genes were downregulated. Currently, this finding further reinforces the idea that the stage-specific

changes in the abundance of TJ-constituting proteins may contribute to the regulation of vitellogenin (VTG) intercellular transport, as suggested by evidence from other bony fish species. In addition, it was observed that the expression of five genes encoding Gap Junction (GJ) proteins showed no significant differences between stages, thus not supporting the hypothesis of GJ proteins participating in the chemical barrier regulating VTG uptake (Table 1).

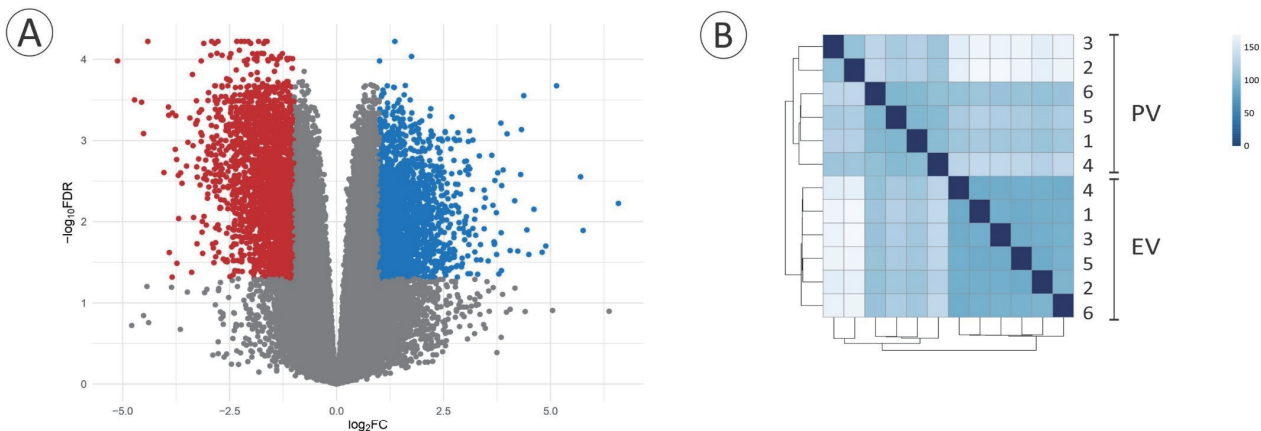


Figure 3. (A) The volcano plot illustrates significant differentially expressed genes between *A. australis* ovarian tissues in the PV and EV stages. Using the defined threshold (q value < 0.05 ; $-1 \geq \log_2FC \geq 1$), a total of 4,878 genes exhibited differential expression among 32,447 genes. Within this group, 2,027 genes displayed downregulation (blue dots), while 2,851 genes demonstrated upregulation (red dots) during the PV-EV transition. (B) The heatmap displays sample clustering based on Euclidean distance. Each sample (numbered 1-6) stands for a biological replicate corresponding to either the PV or the EV stage.

Down-Regulated Genes during the PV-EV Transition		<i>A. anguilla</i> BLAST [†] / HUGo Gene Associated		Log ₂ FC	q Value	PV Reads \pm SEM	EV Reads \pm SEM
Gene ID	TRINITY_ Annotation						
DN13517_c0_g1	claudin-14 [<i>H. sapiens</i>]	claudin-like protein ZF-A9	[XP_035248997.1]/ <i>cldn14</i>	2.24	0.02	45.5 \pm 12.1	14.7 \pm 3.8
DN36018_c0_g1	claudin-3 [<i>R. norvegicus</i>]	claudin-3-like	[XP_035290832.1]/LOC118236501	1.70	0.02	20.8 \pm 4.7	9.8 \pm 2.1
DN7995_c0_g1	MARVELD3 [<i>H. sapiens</i>]	MarvelD3	[XP_035251135.1]/ <i>marveld3</i>	1.22	<0.01	391.3 \pm 20.6	257.5 \pm 36.6
DN5532_c0_g1	claudin-like protein ZF-A89	[D. rerio]	claudin-like protein ZF-A89	1.13	<0.01	542.7 \pm 65.3	356.2 \pm 39.2
DN1688_c0_g3	Jam2a	[D. rerio]	Jam2a	1.12	<0.01	252.2 \pm 13.5	174.2 \pm 8.2
Up-regulated genes during the PV-EV transition							
DN10265_c0_g1	claudin-12	[P. abelii]	claudin-12	-1.03	<0.01	74.5 \pm 14.4	220.3 \pm 10.4
DN4344_c0_g2	MARVELD2	[X. tropicalis]	MarvelD2-like	-1.24	<0.01	92.2 \pm 12.4	323.5 \pm 29.5
Not differentially expressed between PV and EV stages							
DN19581_c0_g1	claudin-7a	[D. rerio]	claudin-7b-like	0.87	0.04	309.3 \pm 20.6	266.8 \pm 42.6
DN2234_c0_g1	claudin-7a	[D. rerio]	claudin-7-a	0.13	0.81	2309.4 \pm 395.7	2580 \pm 490
DN11172_c0_g1	claudin-like protein ZF-A89	[D. rerio]	claudin-like protein ZF-A89	0.37	<0.01	52,673.3 \pm 3,151.4	30,285.6 \pm 1,014.1
DN23602_c0_g2	claudin-8	[M. musculus]	claudin-8-like	-0.43	0.36	10.2 \pm 1.9	22.2 \pm 3.2
DN19953_c0_g1	claudin-11	[B. taurus]	claudin-11a	-0.70	0.08	14.8 \pm 2.4	35.8 \pm 3.6
DN11142_c0_g1	Jam3b	[D. rerio]	Jam3b	-1.13	0.14	16.8 \pm 6.3	55.7 \pm 15.9
DN21932_c0_g1	Jam2a	[D. rerio]	Jam2a	0.59	0.34	10.7 \pm 1.9	11.7 \pm 2.3
DN6434_c0_g1	occludin	[R. norvegicus]	occludin-like	0.24	0.23	877.5 \pm 99.6	958.8 \pm 43.3
DN5516_c0_g1	LSR	[Anguillina-1] [<i>M. musculus</i>]	Lsr	0.31	0.31	623.3 \pm 72.6	698.7 \pm 74.5
DN4811_c0_g1	ILDR1	[Anguillina-2] [<i>X. laevis</i>]	Ildr1a	-0.29	0.07	3746.9 \pm 339.2	5119.4 \pm 317.7
DN9449_c0_g1	ILDR2	[Anguillina-3] [<i>M. musculus</i>]	Ildr2	0.15	0.11	11.2 \pm 0.9	24.6 \pm 1.5
DN198_c0_g1	tight junction ZO-1	[C. familiaris]	tight junction ZO-1-like	-0.48	0.02	1066.7 \pm 132.1	1836.1 \pm 99.2
DN5322_c0_g1	tight junction ZO-1	[C. familiaris]	tight junction ZO-1-like	0.04	0.89	84.3 \pm 5.8	126.5 \pm 10.9
DN7765_c0_g1	tight junction ZO-2	[M. musculus]	tight junction ZO-2-like	0.87	0.01	460.5 \pm 51.0	363.5 \pm 48.4
DN5748_c0_g1	tight junction ZO-3	[H. sapiens]	tight junction ZO-3a	<-0.01	0.99	1619.3 \pm 200.9	1986.6 \pm 124.7
DN2057_c0_g1	tight junction ZO-3	[H. sapiens]	tight junction ZO-3	-0.40	0.03	277.3 \pm 270.3	4170.8 \pm 221.7
DN2926_c0_g1	MARVELD3	[H. sapiens]	MarvelD3	0.33	0.42	525.5 \pm 82.8	584.505 \pm 94.0
DN4344_c0_g1	MARVELD2	[X. tropicalis]	MarvelD2b	-0.1	0.50	1209.8 \pm 100.3	1624.2 \pm 93.8
DN7029_c0_g4	gj gamma 1 protein	[D. rerio]	gj gamma 1 protein-like	-0.31	0.03	787 \pm 81	1270.8 \pm 47.1
DN998_c2_g1	gj beta-3 protein	[R. norvegicus]	gj beta-3 protein-like	-0.15	0.23	5111.3 \pm 429.3	6064.8 \pm 236.4
DN379_c0_g1	gj beta-4 protein	[R. norvegicus]	gj beta-4 protein-like	0.70	<0.01	180.6 \pm 18.3	167.3 \pm 13.1
DN15444_c0_g1	gj beta-7 protein	[H. sapiens]	connexin 28.8	1.27	0.09	36.8 \pm 8.1	24.8 \pm 6.3
DN12469_c0_g1	gj 32.7 protein	[M. undulatus]	connexin 34.5	-0.88	0.02	41.7 \pm 6.1	114.8 \pm 15.3

Table 1. Expression of genes encoding cell junctions in *A. australis* ovarian tissue during transition from the PV to the EV stage

Expression of genes related to receptor-mediated endocytosis mechanism and Vtg processing during the PV-EV transition

Further analysis using RNA-seq was conducted to explore the gene expression associated with VTG recognition, clathrin-mediated endocytosis, molecular mechanism for vesicular trafficking, and VTG protein hydrolysis. In the *A. australis* ovarian transcriptome, two genes encoding putative Vtgrs (from the LDL receptor family: Lr8

and Lrp13) were identified. Notably, their expression showed no significant differences between the EV and PV stages. This finding strengthens the notion that putative Vtgr expression is not a limiting factor for VTG uptake. In the transcriptome, it was observed that, except for the down-regulation of cathepsin L1 and nothepsin gene expression, most cathepsins did not exhibit differential expression between the PV and EV stages. This implies that cathepsins may be regulated after transcription.

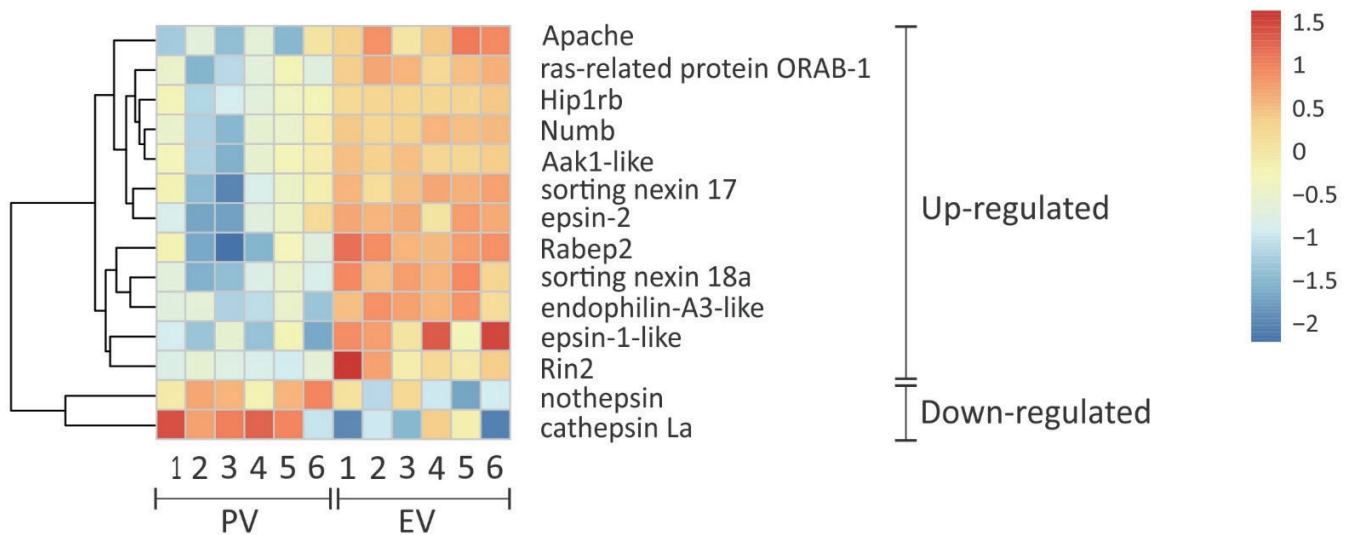


Figure 4. Heatmap depicting differentially expressed genes involved in clathrin-mediated endocytosis, vesicular trafficking, and proteolysis, which may participate in the VTG uptake approach of *A. australis*. Color intensity represents ovarian gene expression comparisons between the PV and EV stages. The color scale gradient, ranging from red to blue, corresponds to high to low gene expression levels. The heatmap illustrates genes that are upregulated and downregulated during the PV-EV transition. Each row represents the expression of a gene across biological replicates from either the PV or EV stage (columns).

Summary

This study identified the differential expression of genes encoding TJ-constituting proteins during the PV-EV transition, indicating their role in regulating VTG intake into the oocyte surface. Genes related to clathrin-mediated endocytosis and vesicular trafficking components were significantly upregulated during the PV-EV transition, suggesting their potential importance in controlling VTG accumulation at the follicle membrane. Additionally, two genes encoding Vtgrs were discovered in the *A. australis*, representing Lr8 and Lrp13 members of the LDL receptor gene family, respectively.

The RNA-Seq strategy in this study utilized the MGIEasy library prep kit and was conducted on the DNBSEQ sequencing platform. DNBSEQ-G400 utilized a brand-new cartridge system, enabling flexible support for various sequencing modes. It featured an optimized optical and biochemical system, allowing full-load PE100 (FCL) sequencing to be completed in approximately 38 hours.



DNBSEQ-G400 Genetic Sequencer

References

1. Babio, L., Lokman, P.M., Damsteegt, E.L. and Dutoit, L. (2022) Are Cell Junctions Implicated in the Regulation of Vitellogenin Uptake? Insights from an RNAseq-Based Study in Eel, *Anguilla australis*. *Cells* 11, 550.
2. Parma, L., Bonaldo, A., Pirini, M., Viroli, C., Parmeggiani, A., Bonvini, E., et al. (2015). Fatty acid composition of eggs and its relationships to egg and larval viability from domesticated common sole (*Solea solea*) breeders. *Reprod. Domest. Anim.* 50, 186–194. doi: 10.1111/rda.12466.
3. Charniauxcotton, H. (1985). Vitellogenesis and its control in *Malacostracan crustacea*. *Am. Zool.* 25, 197–206.
4. Yao, R., Wong, N.K., Zhang, X., Zhu, C. and Chen, T. (2020) Vitellogenin Receptor (VgR) Mediates Oocyte Maturation and Ovarian Development in the Pacific White Shrimp (*Litopenaeus vannamei*). *Frontiers in Physiology* 11, 485.
5. Morini, M., Lafont, A.G., Maugars, G., Baloché, S. and Pérez, L. (2020) Identification and stable expression of vitellogenin receptor through vitellogenesis in the European eel. *animal*, 1-10.

Recommended Ordering Information

Category	Product	Cat. NO.
Instruments	Genetic Sequencer DNBSEQ-G400RS	900-000170-00
	MGISP-100RS Automated Sample Preparation System	900-000206-00
	MGISP-960RS Automated Sample Preparation System	900-000146-00
Software	MegaBOLT Bioinformatics analysis accelerator	900-000555-00
Library Prep	MGIEasy RNA Directional Library Prep Set (16 RXN)	1000006385
Sequencing Reagents	DNBSEQ-G400RS High-throughput Sequencing Set (FCL PE100)	1000016950

MGI Tech Co.,Ltd

Building 11, Beishan Industrial Zone, Yantian District, Shenzhen, CHINA, 518083

The copyright of this brochure is solely owned by MGI Tech Co. Ltd.. The information included in this brochure or part of, including but not limited to interior design, cover design and icons, is strictly forbidden to be reproduced or transmitted in any form, by any means (e.g. electronic, photocopying, recording, translating or otherwise) without the prior written permission by MGI Tech Co., Ltd.. All the trademarks or icons in the brochure are the intellectual property of MGI Tech Co., Ltd. and their respective producers.

Version: October 2023

 +86-4000-688-114

 en.mgi-tech.com

 MGI-service@mgi-tech.com

Authors: Jing Gao, Yang Xiao

Editor-in-Charge: Wang Qiwei

Reviewer: Jiang Yao

1. For StandardMPS and CoolMPS: Unless otherwise informed, StandardMPS and CoolMPS sequencing reagents, and sequencers for use with such reagents are not available in Germany, Spain, UK, Sweden, Belgium, Italy, Finland, Czech Republic, Switzerland, Portugal, Austria and Romania. Unless otherwise informed, StandardMPS sequencing reagents, and sequencers for use with such reagents are not available in Hong Kong. No purchase orders for StandardMPS products will be accepted in the USA until after January 1, 2023.

2. For HotMPS sequencers: This sequencer is only available in selected countries, and its software has been specially configured to be used in conjunction with MGI's HotMPS sequencing reagents exclusively.

3. For HotMPS reagents: This sequencing reagent is only available in selected countries.